CrossMark

Evolution of a beach nourishment project using dredged sand from navigation channel, Dunkirk, northern France

Alexandra Spodar[1] · Arnaud Héquette[1] · Marie-Hélène Ruz[1] · Adrien Cartier[2] ·
Pascal Grégoire[3] · Vincent Sipka[1] · Nicolas Forain[3]

Abstract The largest beach replenishment project ever in France was completed in February 2014 in Dunkirk on the coast of northern France. A volume of 1.5×10^6 m^3 of sand extracted from a navigation channel was placed on the beach to build up a 150 to 300 m wide supratidal platform in front of a dike, called « *Digue des Alliés* », which protects several residential districts of Dunkirk from marine flooding. High resolution topographic surveys were carried out during 2½ years to monitor beach morphological changes, completed by a hydrodynamic field experiment conducted in February 2016. Approximately $-138,200$ m^3 of sand, corresponding to 9.2% of the initial nourishment volume, were eroded over the nourishment area in about 2 years. An obvious decrease in erosion eastward with a shift from erosion to accumulation was observed, suggesting an eastward redistribution of sand. This longshore sand drift is beneficial for the eastward beach of Malo-les-Bains where most of the recreational activities are concentrated. Hydrodynamic measurements showed that waves and wave-induced currents play a major role on the longshore sand redistribution compared to tidal flows. Strong relationships were observed between cumulative offshore wave power and beach volume change during distinct beach survey periods ($R^2 = 0.79$ to 0.87), with more significant correlations for northerly waves. A slight decrease in erosion during the second year compared to the first year after nourishment suggests that the loss of sand should decrease after an initial phase of rapid readjustment of the beach shape towards equilibrium.

Keywords Beach nourishment · Beneficial use of dredged sand · Flood defence · Beach morphodynamics

Introduction

Coastal zones are exposed to a range of coastal hazards including erosion and marine flooding that are likely to worsen in the next decades with predicted sea level rise (Nicholls and Cazenave 2010; Rahmstorf et al. 2012) and possible changes in storminess (Bertin et al. 2013; Ruggiero 2013) associated with climate change (IPCC 2013). The likely increase in frequency of extreme water levels during the next decades due to rising sea level (Haigh et al. 2011; Weisse et al. 2012) should result in increasing shoreline retreat and storm-induced flooding along low-elevated areas (Brown et al. 2013; Kruel 2016). Due to the increasing vulnerability of the coastal zones to coastal hazards, the need for coastal protection will necessarily increase in the future, especially in densely populated areas (Neumann et al. 2015).

Coastal engineering structures such as seawalls, dikes and breakwaters have been extensively used for decades for shoreline stabilization all over the world (Charlier et al. 2005; Kamphuis 2010), but these types of hard coastal protections commonly induce adverse effects on beaches and adjoining shorelines by altering hydrodynamics and sediment transport processes (Sánchez-Badorrey et al. 2008; Guimaraes et al. 2016). Therefore, alternate adaptive strategies involving soft

✉ Alexandra Spodar
    alexandra.spodar@univ-littoral.fr

[1] Laboratoire d'Océanologie et de Géosciences, UMR CNRS 8187, Université Littoral Côte d'Opale, 32 Avenue Foch, 62930 Wimereux, France

[2] GEODUNES, 79 rue Pasteur, 59240 Dunkirk, France

[3] Dunkirk Port, 2505 route de l'écluse Trystram, 59386 Dunkirk, France

🍎 Springer

stabilization techniques, including ecosystem-based coastal protection approaches (Koch et al. 2009; Temmerman et al. 2013), have been increasingly called upon to prevent and mitigate coastal risks. Among soft protection techniques, artificial beach nourishment became a widely used practice during the second half of the twentieth century for coastal protection purposes, but also for restoring or enhancing the recreational values of beaches (e.g., Wiegel 1994; Cai et al. 2010; Cooke et al. 2012; Bird and Lewis 2015). Beach replenishment is also considered to be an effective adaptation strategy to counter sea level rise (Dean and Houston 2016).

Beach nourishment has a long history in the United-States where it progressively became the preferred method of coastal protection (Hall 1952; Leonard et al. 1990b; Trembanis and Pilkey 1998; Valverde et al. 1999; Campbell and Benedet 2006). It is also one of the most extensively used shoreline protection techniques in several European countries (Hanson et al. 2002), notably in Spain (Muñoz-Perez et al. 2001; Silveira et al. 2013), Belgium (Charlier and De Meyer 1995; Mertens et al. 2008) and especially in the Netherlands where beach and shoreface nourishment are regularly carried out all along the coast since the early 1990s under a government policy to maintain the position of the shoreline (Roelse 1990; van Duin et al. 2004; Bakker et al. 2012). Beach and shoreface nourishment operations in the Netherlands have resulted in an annual sediment supply of about 12×10^6 m^3 to the coast (Kabat et al. 2009) and recently a single nourishment project of 21×10^6 m^3, called the Sand Engine, was implemented on the Dutch coast in 2011 with the intention to progressively feed a large stretch of coast under the action of wind, waves and currents (Stive et al. 2013). In France, beach nourishment projects, which began in the 1960s (Hamm et al. 2002), have been comparatively more modest, with a total cumulative volume of beach fills of about 12×10^6 m^3 between the early 1960s and the end of the twentieth century (Hanson et al. 2002).

One of the constraints of beach replenishment is the availability of sand of suitable grain-size (Dean 2002). Another potential limitation is the distance of the sand source, which would ideally be located in the vicinity of the nourishment project in order to minimize operation costs. Sedimentation in navigation channels of seaports requires regular dredging for preventing channel infilling and maintaining ship access to ports. Where sand deposition contributes to channel infilling, the dredging of these sediments may represent an opportunity for beach nourishment within easy reach if the composition of the borrowed sand is comparable to the native beach sand, and provided that the quality characteristics of the nourishment sediment will not have harmful impacts on the beach ecosystem (Speybroeck et al. 2006). Most of the earlier beach nourishment projects in the United-States consisted of fills of opportunity from channel maintenance dredging (Campbell and Benedet 2006) and such practice based on the beneficial use of dredging material is still in use in the United-States and in a number of other countries (Shibutani et al. 2013; Silveira et al. 2013).

The use of channel maintenance dredging material has been also carried out for several years by the Port of Dunkirk, in northern France, for stabilizing rapidly eroding shorelines and for protecting coastal defence structures. The largest of these nourishments took place on a beach bordering a sea dike called "*Digue des Alliés*" (Fig. 1) which protects several districts of the city of Dunkirk from marine flooding. 1.5×10^6 m^3 of dredged sand was placed on the beach to build up a wide supratidal sediment platform for protecting the dike from wave attack and preventing storm-induced flooding. The aim of this paper is to assess the efficiency of this beach nourishment project after a period of 2 ½ years of beach surveys and to evaluate the impacts of hydro-meteorological forcings on the observed morphological changes through in situ hydrodynamic measurements and based on the analysis of offshore wave statistics during the survey period.

Study area

The densely-populated coast of northern France is part of the Flemish coastal plain that essentially consists of reclaimed lands (polders), commonly located below mean high tide, which make them particularly exposed to coastal risks, and notably to marine flooding during storm surges (Rufin-Soler et al. 2008; Crapoulet et al. 2016). Most of the coastal farming lands are protected from marine flooding by coastal dunes (Ruz et al. 2005) while flood protection in urban coastal areas is provided by seawalls and sea dikes. The flat lowlands of the coastal plain are also subject to fluvial inundation and a dense system of canals drains the excess water from the polder to the sea through an outlet canal.

The replenished beach surveyed in this study is located along the *Digue des Alliés* sea dike and constitutes the westernmost part of the beach of the seaside resort of Malo-les-Bains (Fig. 1d). The dike, constructed in 1876, protects several areas of the city of Dunkirk from marine inundation and an outlet canal through which inland freshwater is discharged into the sea (Fig. 1d). The dike was breached during storms in 1949 and in 1953, the latter corresponding to the Great North Sea flood of 1953 that had dramatic impacts along the southern North Sea coasts (McRobie et al. 2005). During this event, two breaches, 200 m and 120 m wide, were cut in the dike that resulted in the inundation of low-lying districts of the city of Dunkirk (Maspataud et al. 2013). The development of the Eastern Port and the construction of jetties protruding seaward during the twentieth century, resulted in the interruption of the eastward-directed longshore drift which induced a sediment deficit on the beaches downdrift that leaded to the construction of two breakwaters in 1978 and one in 1984 seaward of the beach of Malo-les-Bains. Although the breakwaters gave
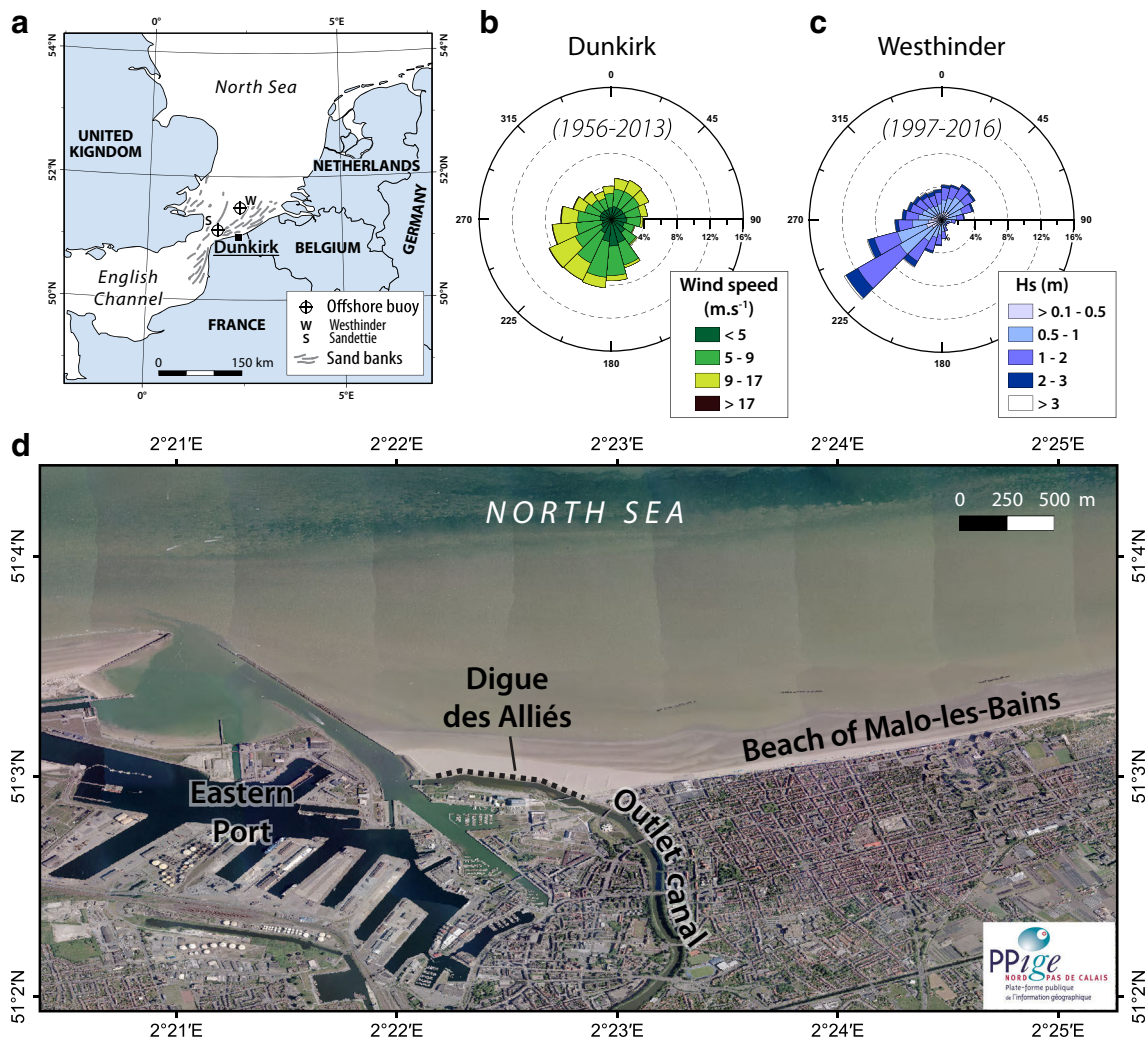
Fig. 1 **a** Location of the study area; **b** Wind rose diagram at Dunkirk based on hourly wind data from Météo-France; **c** Wave rose diagram based on hourly wave measurements at Westhinder wave buoy (see A for location of wave buoy); **d** Aerial photograph of the study site taken in June 2015, 16 months after the completion of the beach nourishment project

satisfactory results, contributing to the beach stability at Malo-les Bains (Oblinger and Anthony 2008), the beach in front of the dike has experienced chronic erosion since then.

The beach bordering the dike and the seawall promenade of Malo-les-Bains (Fig. 1d) is 350 to 400 m wide at low tide and presents a bar-trough morphology across a very gently sloping foreshore (tanβ ≈ 0.012 to 0.015), typical of the macrotidal beaches of the region (Reichmüth and Anthony 2007). The beach is composed of well -to very well-sorted fine sand (mean grain size: 0.14 to 0.24 mm) (DHI 2012). Winds mainly come from the southwest and northeast, but the strongest winds mostly originate from west to southwest (Fig. 1b). Associated with these winds, the wave regime is dominated by waves from southwest to west, originating from the English Channel, followed by waves from the northeast to north, generated in the North Sea (Fig. 1c). Most waves have a significant height of less than 1 m and periods ranging from

4 to 8 s, but wave height may episodically exceed 5 m with periods of 9 to 10 s during major storms (http://candhis.cetmef.developpement-durable.gouv.fr/campagne/). Wave heights are much lower at the coast, however, due to significant wave refraction and energy dissipation over the offshore sand banks and low gradient inner shelf and shoreface (Héquette and Cartier 2016). The tidal regime is semi-diurnal and macrotidal with a spring tidal range of 5. 45 m at Dunkirk. This large tidal range is responsible for relatively strong tidal currents that flow almost parallel to the shoreline, the ebb being directed westward and the flood flowing eastward (Héquette et al. 2008a). Due to a flood-dominated asymmetry in the tidal currents, and because the prevailaing winds and waves originate from the southwest, the net sediment transport is directed to the east-northeast both in the nearshore (Héquette et al. 2008a) and the intertidal zones (Cartier and Héquette 2011).

The beach nourishment project

Given the risk of another failure of the *Digue des Alliés* dike, which showed damage in places, and in order to fulfil the legal requirements to strengthen coastal protection structures following the fateful storm Xynthia in 2010 (Le Louarn 2012), the Port of Dunkirk was commissioned by the French government to reinforce the dike. In order to protect the dike from wave impacts and prevent marine flooding during storms, a massive beach nourishment project was implemented. In addition to creating a buffer zone that would dissipate wave energy and reduce storm surges, the other objectives of the beach replenishment scheme include the beneficial reuse of clean dredging sand, and the potential redistribution of some of the nourishment sediment on downdrift sections of the beach where recreational activities are concentrated.

The design of the project was conducted by DHI-INGEROP (DHI 2012) who carried out numerical modelling based on a two-dimensional morphological model including wave, current and sediment transport, and a simple one-line model for coastline evolution (Grunnet et al. 2012). The beach nourishment was designed for a 50-year return period storm and taking into account a sea level rise of 60 cm by 2100 due to climate change (IPCC 2013), which corresponds to a maximum water level of 7.93 m above Hydrographic Datum (HD).

The borrowed sand was dredged in the access channel of the Eastern port at approximately 1.5 km from the native beach. Analyses of the compatibility of the sediment from the borrow source with the sand of the native beach showed that the grain size was coarser in the dredging area (average median grain size (D_{50}) = 0.27 mm) than on the beach (mean D_{50} = 0.17 mm). Physicochemical analyses, including metal concentration, polycyclic aromatic hydrocarbons (PCB) content and polychlorinated biphenyls (PCB) content, were also realized and validate that the sediment quality met the requirements of the French legislation for a use for beach nourishment.

The sand was extracted from the navigation channel by a trailing suction hopper dredger and was pumped through pipes to the native beach. A total volume of 1.5×10^6 m^3 of sand was placed on the beach, down to approximately the mean low tide limit, during two operations: the first one in December 2011 when 300,000 m^3 were deposited on the beach, followed by a sand placement of 1.2×10^6 m^3 in February 2014 (Cartier et al., 2014). Fig. 2 shows an overview of the morphological evolution of the beach. A topo-bathymetric survey conducted in June 2011 shows the initial beach morphology (Fig. 2a). Before the first beach nourishment operation, the beach was almost completely submerged at high tide as the maximum altitude of the beach hardly exceeded +4 m above HD which is significantly lower than the mean high water spring tide level (MHWS) that reaches +6.05 m above HD. Consequently, the toe of the dike was
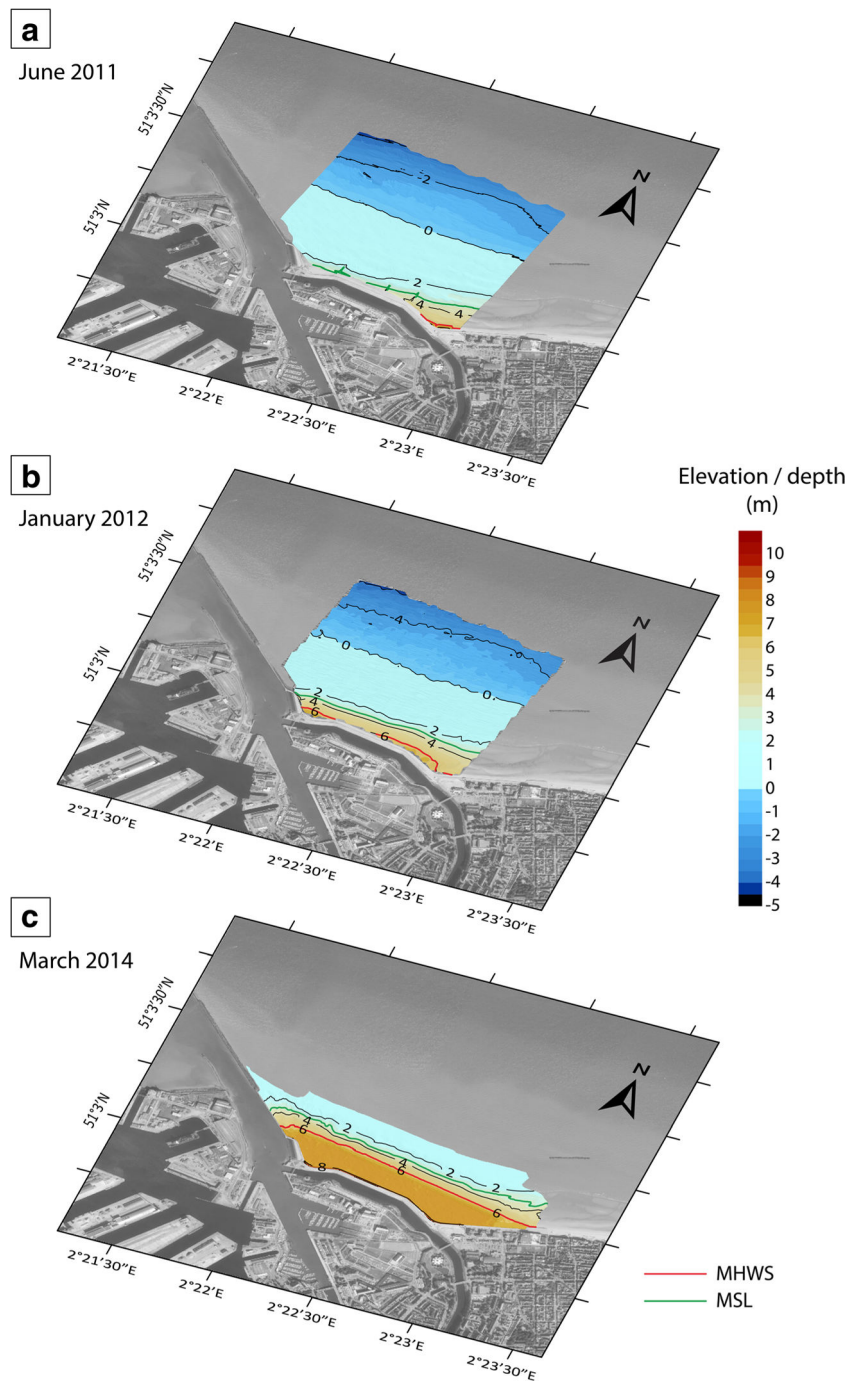
reached by waves at high tide along most of its length. In December 2011, the first nourishment was carried out (Fig. 2b) which resulted in a supply of 300,000 m^3 sand placed at the base of the dike. This first sand supply was an emergency operation to protect the structure against possible storms during winter 2011–2012. This sands supply was responsible for an increase of the level of the upper beach to +6 m above HD over a width of 20 m to 70 m over a length of 1000 m. During the second nourishment operation in February 2014, 1.2×10^6 m^3 of sand were placed over a shoreline length of about 1500 m, which resulted in the creation of a sandy supratidal platform at about +7.6 m above HD (Fig. 3). The supratidal platform reached a width of approximately 300 m in the western part of the nourished beach, 150 m in the central part and 200 m in the eastern part, representing an additional asset for recreational activities. After completion of the second nourishment, the slope of the intertidal beach was approximately 3%.

Methodology

High resolution topographic surveys of the supratidal platform and intertidal beach were carried out after the completion of the beach nourishment to monitor the morphological evolution of the replenished beach. A total of five extensive topographic surveys were conducted in March 2014, October 2014, February 2015, September 2015 and February 2016. The first two surveys were completed over area 1 only (Fig. 4), which corresponds to the nourishment zone that covers a surface area of approximately 0.57 km^2. Since 2015, the survey zone has been extended 2 km eastward, resulting in a surveyed area of about 1.33 km^2. Topographic surveying was carried out using a very high resolution Differential Global Positioning System (DGPS) mounted on a 4WD quad bike, with horizontal and vertical error margins of +/− 2 cm and +/− 4 cm respectively, which resulted in the acquisition of topographic data points with a density ranging from about 34,000 to 42,200 points km^{-2} during the different surveys. These data points were used to create Digital Terrain Models (DTM) using Golden Software Surfer™. The DTMs were obtained by linear interpolation using a Delaunay triangulation resulting in an equidistant grid with a spacing of 2 m.

Nine topographic cross-shore profiles were also surveyed at a higher frequency since February 2015 across the beach nourishment area (Fig. 4) in order to gain a better insight into the short-term morphological dynamics of the nourished beach. Each beach profile was surveyed thirteen times from 20 February 2015 to 28 July 2016. These profiles were complemented by topographic profiles extracted from the DTMs of March 2014 and October 2014, resulting in a series of fifteen consecutive profiles spanning over the entire post-nourishment period. Overall, seven profile surveys were

Fig. 2 a Bed elevation of the initial beach in June 2011, **b** in January 2012 (after the first nourishment operation of December 2011), and **c** in March 2014 (after the completion of the beach nourishment in February 2014). MHWS is mean high water spring level and MSL is mean sea level. The topo-bathymetric data of 2011 and 2012 were collected by HydroConsult (2011) and by GPMD (2012) respectively

measured during summer and eight during winter. The successive topographic surveys of beach profiles allowed the computation of net (V_n) and gross (V_g) volume changes according to the following the equations:

$$V_n = |V_a - V_e| \tag{1}$$

$$V_g = |V_a| + |V_e| \tag{2}$$

where V_a is the volume of accretion and V_e the volume of erosion in a beach profile. The sediment volume change (V_n and V_g) was calculated for each individual cross-shore profile between two dates. Due to differences in cross-shore profile length, volume changes have been normalized by the profile length. All the volumes per meter ($m^3 \, m^{-1}$) were then averaged to give a mean value for the entire study area.

A hydrodynamic field experiment was carried out from 10 to 17 February 2016. One Acoustic Doppler Current Profiler (ADCP) was moored in the nearshore zone in a water depth of about −4.1 m below HD and two

Fig. 3 Photographs of the beach bordering the *Digue des Alliés* dike (**a**) before and (**b**) two months after the completion of the beach nourishment

electromagnetic wave and current meters (Midas Valeport©) were deployed on the lower beach (Fig. 4). CM 1 was placed on the eastern part of the beach nourishment at 1.1 m above HD and CM2 on the western part at 2.2 m above HD. These instruments recorded data at a frequency of 2 Hz during 9 min intervals every 15 min. The duration of each burst of hydrodynamic measurements was chosen as a compromise between two opposite constraints. It had to be long enough to allow wave spectral analysis, but it also had to be short enough to respect stationary conditions as water depth is continuously changing over a tidal cycle on macrotidal beaches. Wave characteristics were obtained by spectral analysis, providing almost continuous records of significant wave height (H_s), wave period (T_p), and water depth (h). Wave directions were also obtained from the ADCP data, but not from the electromagnetic current meters that only provide non-directional wave measurements. Since the electromagnetic current meters were located on the beach, wave direction was considered to be shore-normal due to refraction. All instruments recorded mean current velocity and direction, as well as longshore and cross-shore current velocities with an accuracy of 0.02 m.s^{-1}. Current velocities were measured at different elevations above seabed depending on the instrument. Electronic wave and current meters recorded velocity
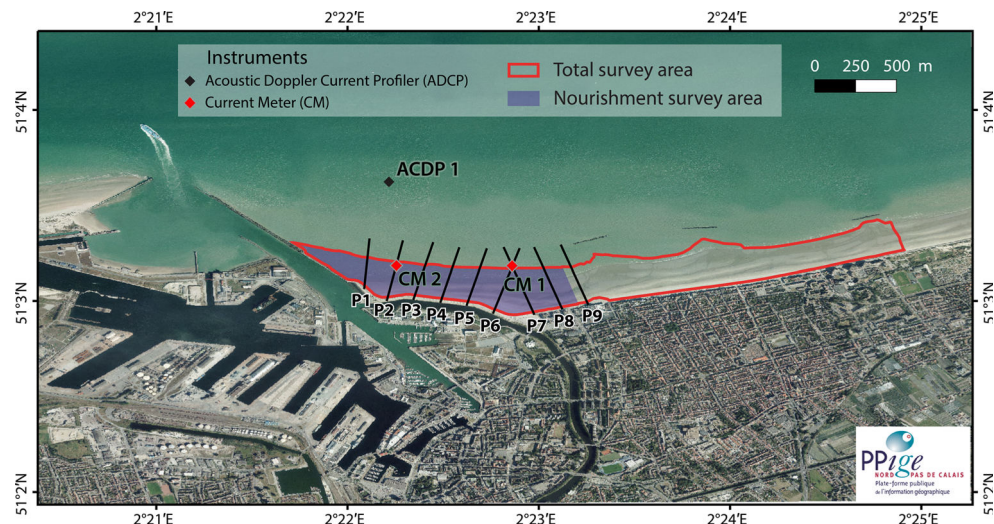
at 0.2 m above seabed while the ADCP measured current at intervals cells of 0.2 m through the water column from 0.83 m above seabed to the water surface. For the ADCP, current velocity at 0.2 m was calculated by applying a logarithmic regression curve to the measured velocities obtained at different elevations in the water column.

Sediment samples were collected in the vicinity of the three instruments and were analyzed using a laser granulometer which provided the median grain size (D_{50}). In order to estimate the initiation of sediment transport, the combined wave and current flow shear velocity shear velocity (u_{*cw}) was calculated according to the algorithms developed by Grant and Madsen ([1986]) for interaction of unidirectional and wave-induced oscillatory flows in the bottom boundary layer. This procedure requires the calculation of a combined flow friction factor (f_{cw}) obtained from:

$$\frac{1}{(4f_{cw}^{0.5})} + log\left[\frac{1}{(4f_{cw}^{0.5})}\right] = log\left(\frac{C_r u_b}{w z_0}\right) + 0.14\left(4f_{cw}^{0.5}\right) - 1.65 \quad (3)$$

where u_b is the maximum near-bed wave orbital velocity calculated from linear wave theory, w is the radian wave frequency ($2\pi/T$), z_0 is the bottom roughness related to the bottom roughness height, k_b, by $z_0 = k_b / 30$ and C_r is the wave to current strength ratio. Effective combined skin friction shear

Fig. 4 Location of the two areas of topographic survey, the beach profiles, and the hydrographic instruments (ADCP, CM1, CM2) during the February 2016 field experiment. Area 1 corresponds to the zone of beach nourishment. The aerial photograph of 2012 shows the configuration of the beach prior to the beach nourishment

velocity is then calculated from the vector addition of the enhanced current and wave shear stress components separated by an angle θ:

$$u_{*cw} = u_{*wm}\left[1 + 2(u_{*c}/u_{*wm})^2 cos\theta + (u_{*c}/u_{*wm})^4\right]^{0,25} \quad (4)$$

where u_{*wm} is the maximum wave shear velocity and u_{*c} is the current shear velocity. Threshold for sediment motion was evaluated by calculating a critical shear velocity (u_{*cr}) using the Yalin method to obtain the dimensionless critical Shields parameter θ_{cr}. The θ_{cr} value is then used to calculate the critical bed shear stress τ_{cr} from:

$$\tau_{cr} = \theta_{cr}(\rho_s - \rho)gD_{50} \quad (5)$$

where ρ_s and ρ are the sediment and fluid density respectively, and g is the acceleration due to gravity. The critical shear velocity u_{*cr} is finally obtained from the quadratic law as:

$$u_{*cr} = \left(\tau_{cr}/\rho\right)^{0.5} \quad (6)$$

More details about the calculation procedures of the combined flow shear velocity and critical shear velocity can be found in Héquette et al. (2008b).

Meteorological conditions during the survey period were analysed using hourly wind data (speed and direction) from *Météo France* weather station in Dunkirk and from the Sandettie Lightship buoy located approximately 16 km offshore (Fig. 1). Directional wave data have been measured for years at the Westhinder wave buoy offshore of the study site (Fig. 1), but unfortunately no data were recorded during the field experiment conducted between 10 and 17 February 2016. There are also numerous data gaps in the records between March 2014 and July 2016, which corresponds to the period of our beach surveys. Non-directional significant wave height and period measured at the Sandettie wave buoy were alternatively used for analyzing the potential impacts of wave forcing on the replenished beach. Hourly wave data recorded over 29 months (1 March 2014 to 28 July 2016) at the Sandettie Lightship buoy were used to compute the average offshore wave power $\overline{P}$ and the cumulative wave power P_c between consecutive beach surveys according to the following formulae:

$$P_c = \sum \frac{1}{16}\rho g H_s^2 c_g \quad (7)$$

$$\overline{P} = \frac{1}{16}\rho g H_s^2 c_g \quad (8)$$

where ρ is the density of seawater in kg m^{-3}, g the gravitational acceleration in m s^{-2} and C_g the wave group velocity in m s^{-1} determined from linear wave theory using the measured wave period.
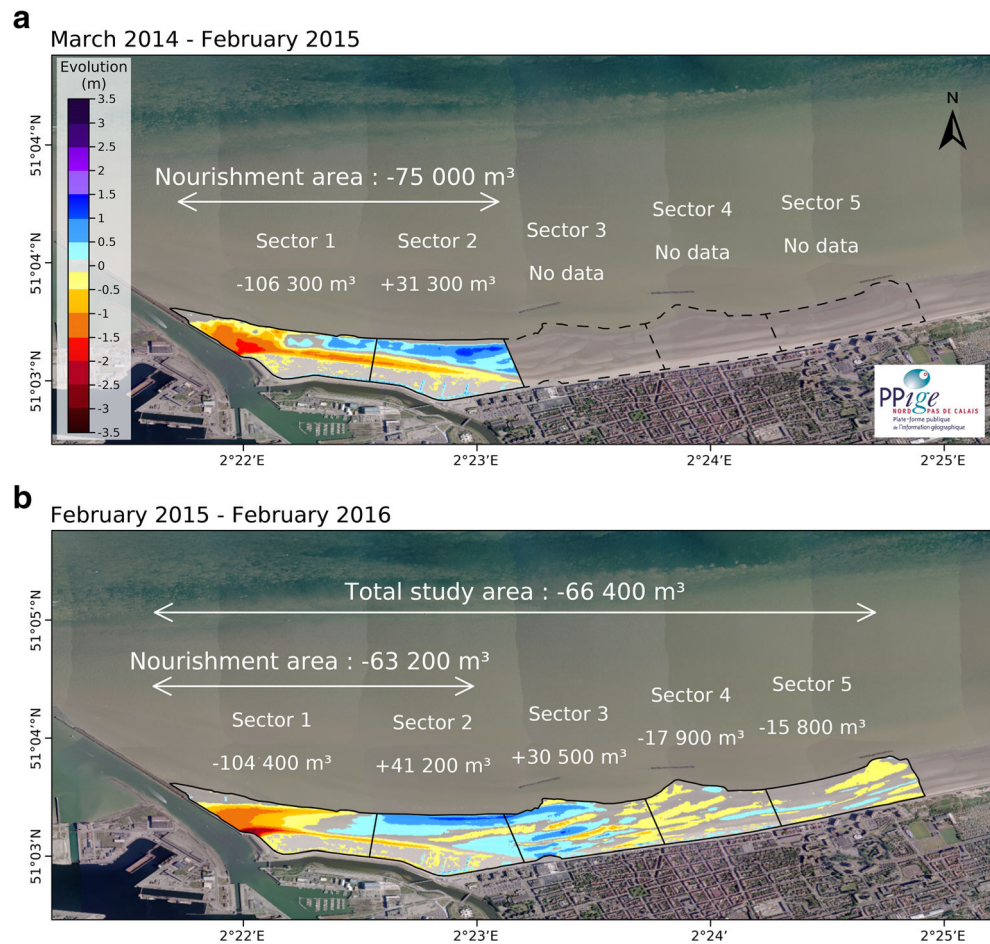
Morphological evolution of the beach nourishment

The morphological changes of the beach during the survey period between March 2014 and February 2016 are shown in Fig. 5. A loss of approximately −138,000 m^3 of sand was measured over the nourishment area (sectors 1 and 2, Fig. 5 & Table 1) which corresponds to 9.2% of the total volume of beach fill. During the first year after the completion of the beach replenishment project, significant erosion took place in the western part of sand emplacement with a loss of about −106,300 m^3 over sector 1 whereas an accumulation of more than 31,000 m^3 was observed in sector 2 (Fig. 5a), suggesting an eastward sediment transport. Overall, a sediment volume of about 75,000 m^3 was eroded from the nourishment area during the first year, representing approximately 5% of the sand placement. It is noteworthy that the most significant erosion occurred in winter between October 2014 and February 2015 with a net loss of - 65,600 m^3 (−0.11 m^3 m^{-2}), whereas between March and October 2014 merely 9400 m^3 (−0.02 m^3 m^{-2}) were eroded.

When looking in more detail at the morphological variations of the beach, one can see that both erosion and accumulation occurred in both sectors during the first year of beach monitoring. Except for the westernmost part of the beach nourishment area where erosion was extensive, erosion mostly affected the edge of the supratidal platform while the lower beach experienced sediment accumulation (Fig. 5a). A large proportion of the supratidal platform remained stable during that period with only small areas of limited erosion (<0.2 m) (Fig. 5a), which are due to aeolian deflation that was responsible for alongshore and onshore sand transport. Because some of this sand was accumulating on the street and parking lots backing the dike, sand fences were installed in December 2014 on the supra tidal platform in sector 2 to trap wind-blown sand and limit landward aeolian transport of beach sand. Localized sand deposition along these sand fences is observable in sector 2 in the form of thin linear accumulations on the supratidal platform (Fig. 5a).

During the second monitoring year, similar spatial patterns of morphological change were observed in the nourishment area with a loss of - 104,400 m^3 in sector 1 and a gain of +41,200 m^3 in sector 2 (Fig. 5b), which represents a net erosion of - 63,200 m^3 corresponding to 4.2% of the total sand volume initially emplaced. Again, erosion was predominantly limited to the western part of the nourishment area and to the edge of the supratidal platform. Sediment accumulation was largely restricted to sector 2 and mostly over the lower beach (Fig. 5b). As for the first year of survey, most of the erosion occurred during winter (−62,400 m^3 between September 2015 and February 2016) whereas negligible erosion was measured during the spring and summer months (− 800 m^3 from February to September 2015) (Table 1). Our results suggest that erosion of the replenished beach was slightly lower during

Fig. 5 Sediment volume change
in the different surveys areas of
the surveyed beach between (**a**)
March 2014 and February 2015
and between (**b**) March 2015 and
February 2016

the second year, decreasing from - 75,000 m^3 (-0.13 m^3 m^{-2})
to - 63,200 m^3 (-0.11 m^3 m^{-2}).

The topographic surveys were extending eastward along
the dike of Malo-les-Bains during the second monitoring year.
The sediment budget of the total survey area is negative with a
loss of 66,400 m^3 between February 2015 and February 2016
(Fig. 5b). The summer period was characterized by a positive
sediment budget of about +19,000 m^3 while a loss of approx-
imately - 85,000 m^3 of sand was observed during winter
(Table 1). As previously mentioned, most of the erosion took
place in the western part of the nourishment area with a loss of
- 104,400 m^3 during the second year of beach monitoring
(Fig. 5b), but this erosion was partly compensated for by an
accumulation of +71,700 m^3 in sectors 2 and 3 (Fig. 5b,
Table 1), suggesting again an eastward redistribution of sand.

The cross-shore topographic profiles surveyed until
July 2016 show the same tendencies (Fig. 6). The net volume
changes computed for each profile between March 2014 and
July 2016 clearly show the significant erosion of the western
part of the nourished area, with a net volume change of more
than - 500 m^3 m^{-1} along Profile 1 (Fig. 6a). There is an obvi-
ous decrease in erosion eastward with a shift from erosion to
accumulation between Profile 4 and 5. Accretion increases

eastward from Profile 5, reaching +284 m^3 m^{-1} on Profile 9
(Fig. 6a). All profiles show significant changes in morphology
and/or slope during the monitoring period (Fig. 6 b-d). Profile
1, to the west, essentially experienced landward retreat due to
continuous erosion and progressive slope decrease from 3.0%
in March 2014 to 2.1% in July 2016 as the foreshore profile
evolved towards equilibrium (Fig. 6b). In the central part of
the nourishment area, Profile 5 underwent both erosion and
accumulation, with a loss of about 102 m^3 m^{-1} on the upper
beach and a gain of nearly 155 m^3 m^{-1} on the middle and the
lower beach (Fig. 6c), resulting in a net accumulation of ap-
proximately 53 m^3 m^{-1}. The slope of the foreshore also de-
creased in that area of the beach from 2.9% in March 2014 to
1.53% in July 2016, which nearly corresponds to the theoret-
ical equilibrium profile slope of 1.42% determined for the
beach nourishment from numerical modelling (DHI, 2012).
Profile 9, at the eastern limit of the nourishment, shows a
continuous accretion since June 2011 (Fig. 6d), presumably
due to the longshore redistribution of some of the nourishment
sand to the east. Although beach slope was fairly constant
during the 2014–2016 monitoring period, ranging from 1.27
to 1.29%, the beach morphology was highly variable with the
progressive development and movement of intertidal bars. It is

Table 1 Changes in the sediment volume of the nourished beach between March 2014 and February 2016 computed from differential DTMs

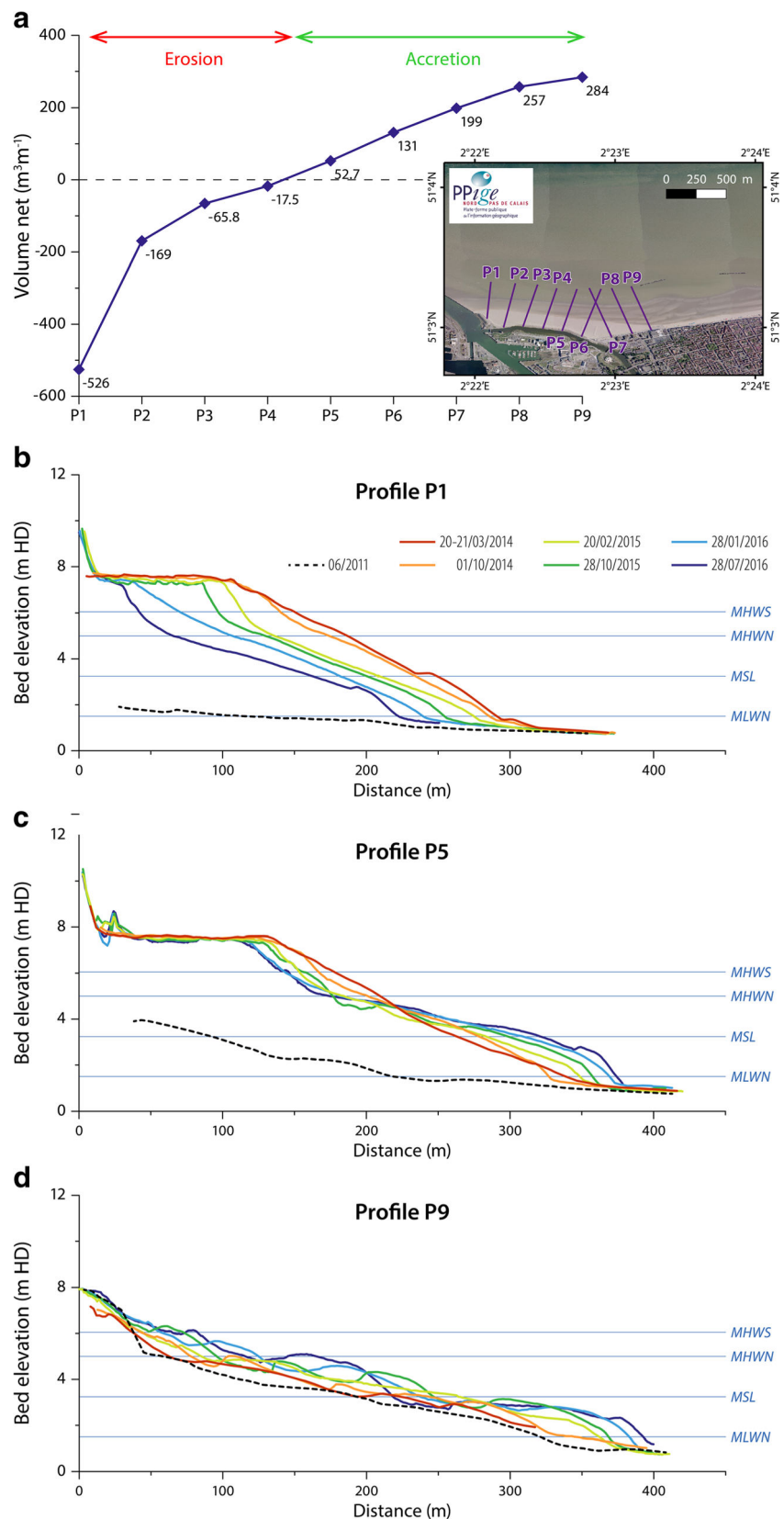|		Sector 1		Sector 2		Sector 3		Sector 4		Sector 5		Nourishment Area (Sector 1 + sector 2)		Total area (All the sectors)
Surface area (m²)		276,400		296,600		287,800		235,800		232,700		572,000		1,328,200
Volume change (m³) (m³ m⁻²)	03/2014–10/2014	−26,800	−0.10	17,400	0.06	—	—	—	—	—	—	−9400	−0.02	—
	10/2014–02/2015	−79,500	−0.29	13,900	0.05	—	—	—	—	—	—	−65,600	−0.11	—
	02/2015–09/2015	−31,000	−0.11	30,200	0.10	17,800	0.06	1000	0.00	900	0.00	−800	0.00	18,900
	09/2015–02/2016	−73,400	−0.27	11,000	0.04	12,700	0.05	−18,900	−0.08	−16,700	−0.07	−62,400	−0.11	−85,300
Total (m³) (m³ m⁻²)	03/2014–02/2016	−210,700	−0.76	72,500	0.24	—	—	—	—	—	—	−138,200	−0.24	—

noteworthy that a barred morphology developed with increasing sand volume on the beach, conversely to the western and central parts of the surveyed area where bar development was virtually absent, showing that intertidal bar only form where sediment supply is sufficient.

Analyses of nearshore and beach hydrodynamics

During the field experiment that was carried out from 10 to 17 February 2016, wind speed was generally moderate with a mean wind speed of 6 m s⁻¹ at Dunkirk. Nevertheless, a distinct northeasterly wind event occurred on 14 and 15 February during which mean wind speed was 9.7 m s⁻¹ with a maximum wind of about 13 m s⁻¹ recorded on 15 February (Fig. 7a). During this event, offshore significant wave heights (H_s) of 3.3 m were observed at the Sandettie wave buoy which was significantly higher than the other H_s recorded during the experiment (Fig. 7b). Due to significant energy dissipation over the inner shelf and nearshore sand banks, wave heights were considerably lower near the coast as the maximum H_s measured in the nearshore zone reached only 1.92 m. The low gradient nearshore slope was responsible for further energy dissipation of the incident waves up to the beach where H_s was always lower than in the nearshore zone, with a maximum H_s of 1.78 m measured on the lower beach by the CM2 instrument (Fig. 7b).

The analyses of the mean near-bed current velocities ($z = 0.2$ m) showed a typical flood-dominated asymmetry (Fig. 7d). This is particularly obvious in the nearshore zone where the velocities of the easterly-directed flood currents were significantly higher than those of the ebb currents (Figs. 7d & 8a). Although the current meters deployed on the beach were emerged during several hours during each tide, current velocities were generally higher during flood compared to ebb (Fig. 8a). Current speeds were higher in the nearshore zone reaching a maximum velocity of 0.62 m s⁻¹ during spring tide at the beginning of the field experiment whereas a maximum current velocity of only 0.43 m s⁻¹ was recorded on the lower beach (Fig. 7d). The semi-diurnal fluctuations in current velocities in the nearshore zone clearly show that the circulation is tidally modulated with a general decrease in current velocity with decreasing tidal range. Near-bed current velocities on the lower beach show more irregular variations due to a combination of tidal and wave forcing. Wave forcing appears particularly important on the beach since the highest current velocities were not recorded during the largest tides, conversely to what was observed in the nearshore zone, but during the wind event of 14–15 February when the higher waves were recorded (Figs. 7 d & b). Interestingly, the variations in cross-shore current velocities indicate that the regular symmetric pattern of alternating onshore- and offshore-directed currents was no longer
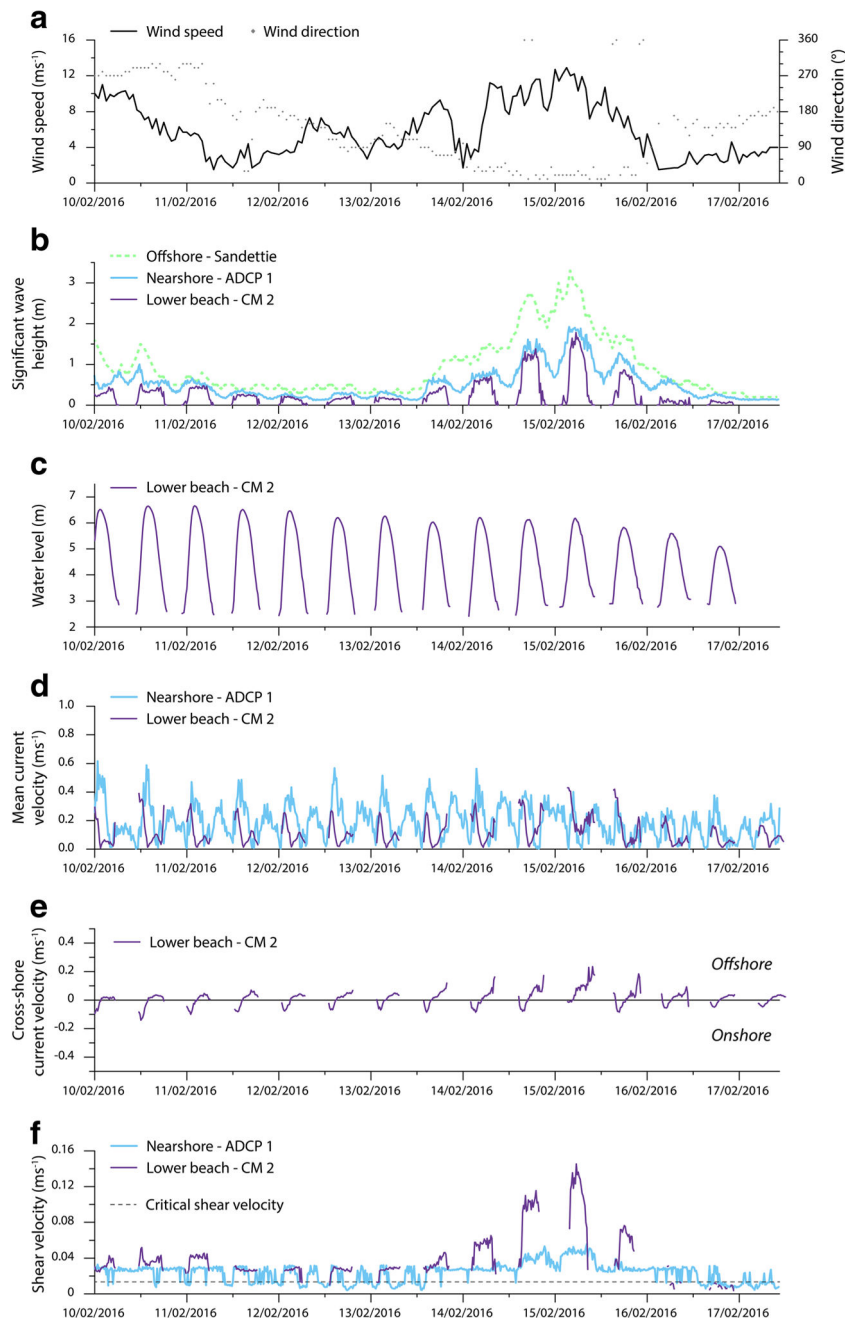
Fig. 6 (a) Net volume change per unit length of coastline for each beach profile between March 2014 and July 2016; (b-d) Evolution of selected cross-shore profiles between June 2011 and July 2016. MHWS is mean high water spring level, MSL is mean sea level, and MHWN and MLWN are mean high water and mean low water at neap tide. The 2011 topographic data were collected by HydroConsult (2011)

occurring during the 14–15 February wind event when cross-shore currents were dominantly flowing offshore (Fig. 7e). During this event, an offshore-directed component of the mean flow was recorded by both current

Fig. 7 Time-series of wind and hydrodynamic parameters measured during the field experiment from 10 to 17 February 2016: (**a**) hourly wind speed and direction in Dunkirk (source: Meteo-France), (**b**) significant wave height (H_s) in deep water, nearshore zone and on the lower beach, (**c**) water depth on the lower beach (relative to Hydrographic Datum), (**d**) mean (non-directional) near-bed current velocity ($z = 0.2$ m), (**e**) cross-shore current velocity on the lower beach, and (**f**) combined wave-current shear velocity. The location of the instruments is indicated in Fig. 2
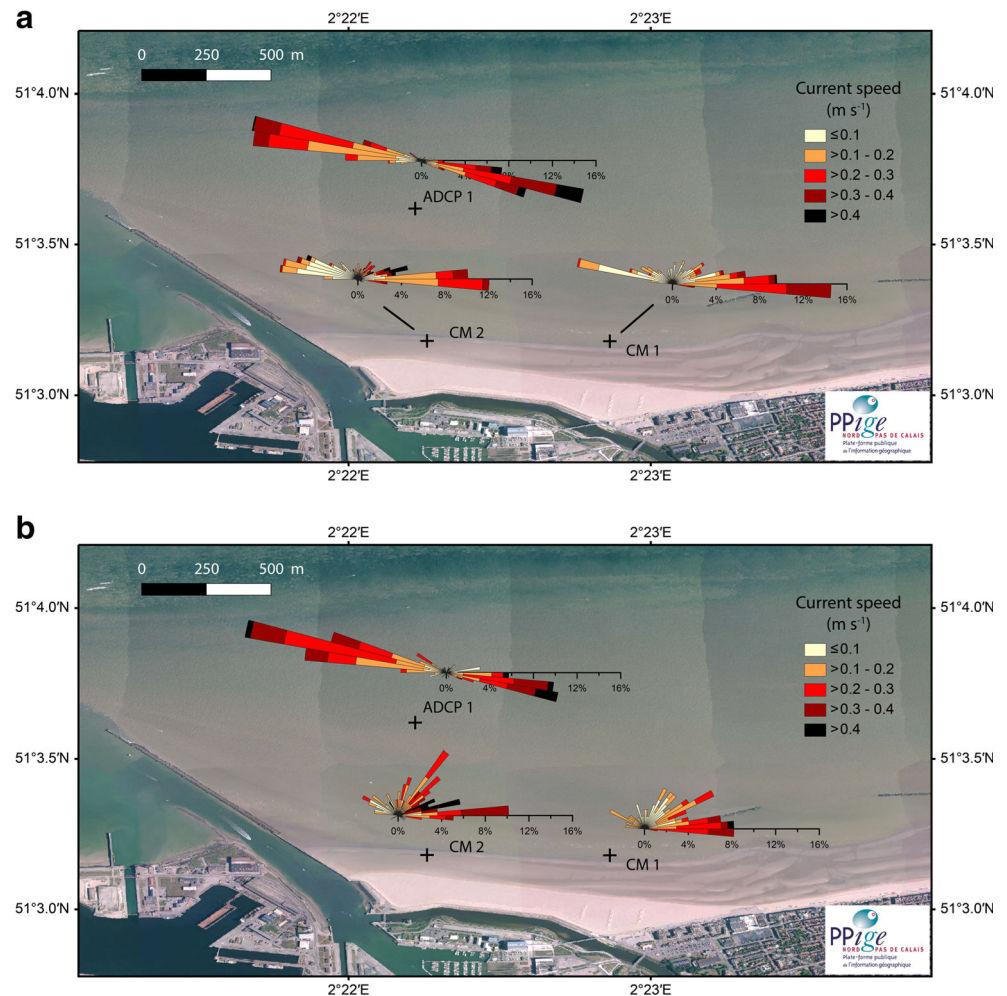

meters on the lower beach (Fig. 8b), presumably due to storm-induced return flows.

The calculation of combined flow shear velocities (u_{*cw}) highlights the importance of waves and wave-induced flows on total bed stress comparatively to tidal flows, particularly on the lower beach where the contribution of waves is very significant due to shallow water depths in comparison to the nearshore zone (Fig. 7f). The relatively lower contribution of tidal flows on bed shear stress on the lower beach compared to the nearshore zone is also explained by the gradual shoreward decrease in tidal current strength as water depths become shallower. Based on the median grain diameter of the bottom

sediments collected near the ADCP ($D_{50} = 0.24$ mm) and the CM2 current meter ($D_{50} = 0.25$ mm), the critical shear velocity (u_{*cr}) for the initiation of sediment motion is 0.013 m s^{-1} both in the nearshore zone and on the lower beach (Fig. 7f). Our results show that sediment transport likely occurred during all tidal cycles in the nearshore zone, but also suggest that there was no transport during slack tides. A notable increase in u_{*cw} is observed during the 14–15 February wind event, related to higher wave-induced bed shear stress. On the lower beach, however, the combined flow shear velocity virtually always exceeded u_{*cr}, suggesting almost continuous sediment transport as soon as the beach was submerged (Fig. 7f). On 14
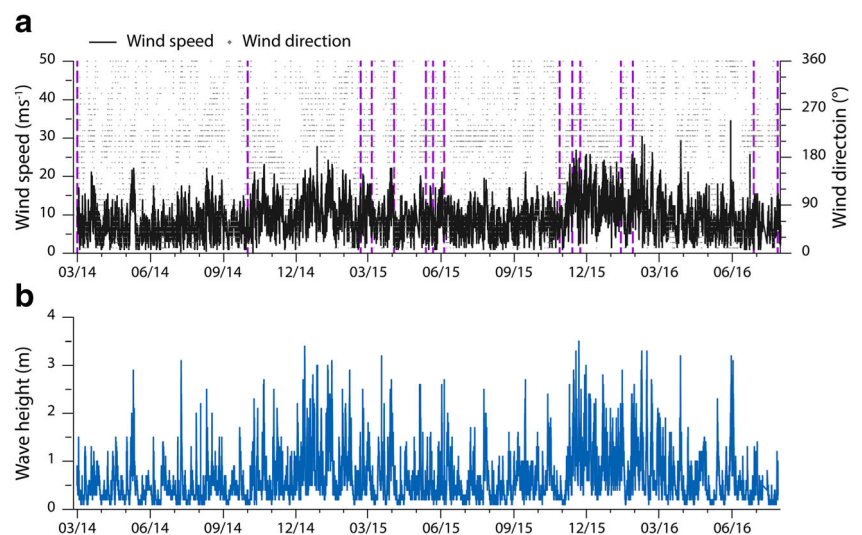
Fig. 8 Directional distribution of mean currents (**a**) during the entire field experiment from 10 to 17 February 2016 and (**b**) during the wind event of 14–15 February 2016

and 15 February, u_{*cw} considerably increased on the lower beach in response to large wave orbital motions in shallow water depths, which probably resulted in very significant sediment transport to the east and obliquely seaward (Fig. 8b).

Conversely, u_{*cw} was lower than u_{*cr} after the wind event on 16 and 17 February, which suggests that tidal currents alone can hardly induce sediment transport on the beach in the absence of waves.

Fig. 9 Hourly (**a**) wind speed and direction, and (**b**) significant wave height (H_s) measured at the Sandettie Lightship wave buoy from March 2014 to July 2016. See Fig. 1 for the location of the measurement station. The dashed vertical lines correspond to the dates of the topographic beach surveys

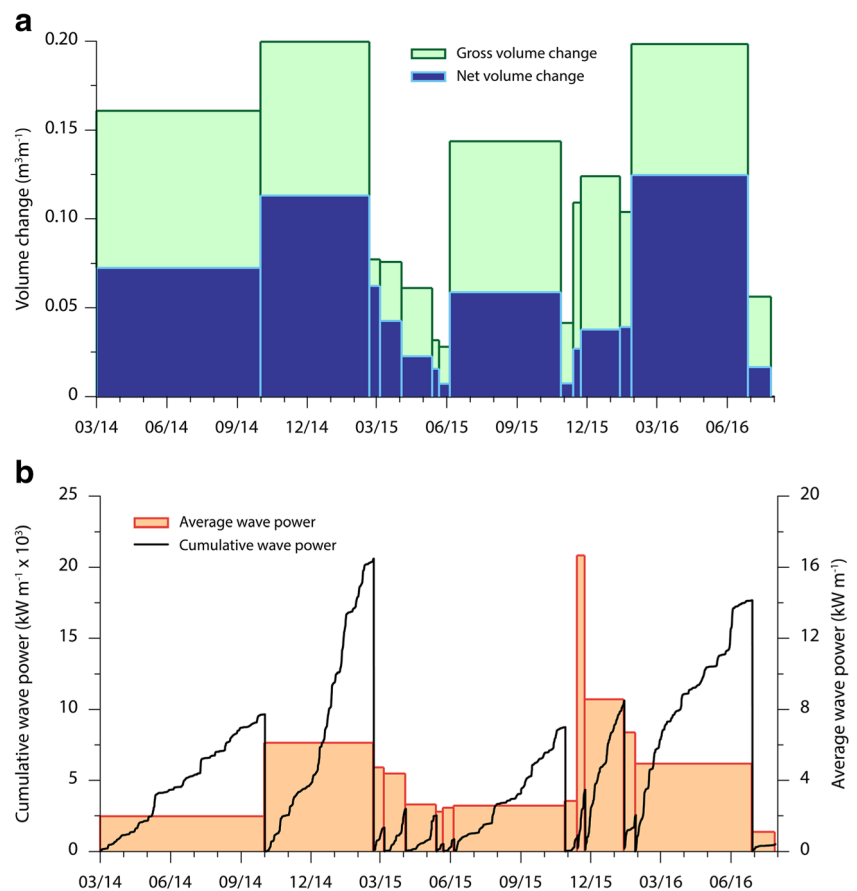## Impacts of wind and wave forcing on the evolution of the nourished beach

Offshore wind and wave data recorded at the Sandettie Lightship buoy between 1 March 2014 and 28 July 2016 were used to assess the response of the beach to hydro-meteorological forcing since the completion of the beach replenishment project. Although the period 2014–2016 was not particularly stormy or characterized by violent storms, 7% of the winds had speeds ≥ 16 m s^{-1} while weak to moderate winds (≤ 8 m s^{-1}) represented 43% of the observations (Fig. 9a). Most winds originated from the southwest quadrant (55%) followed by winds from the northeast (19%) which closely corresponds to the wind regime in the region (Fig. 1b). These winds generated waves with significant heights up to 3.5 m that, similarly to the strongest winds, mainly occurred during winter (Fig. 9b).

High velocity winds and associated high amplitude offshore wave heights predominantly occurred during the winter months (Fig. 9 a & b), notably between October 2014 and February 2015 (34% of winds with speeds ≥ 12 m s^{-1}) and especially from November 2015 to March 2016 (41% of winds with speeds ≥ 12 m s^{-1}). Although most of these strong

winds were blowing from the southwest during both periods, a higher proportion of northeasterly winds were recorded during the second winter (14%) compared to the first winter (9%). The variability in wind speed and wave height during the beach monitoring period can hardly explain the observed changes in sediment volume of the nourished beach, because more significant volume changes were measured during the first year of beach monitoring (Table 1) that was characterized by a lower frequency of high velocity winds and lower significant wave heights during the winter months (mean $H_s = 0.79$ m) compared to the 2015–2016 winter period (mean $H_s = 0.87$ m).

Although higher eroded volumes during the first year may be related to a more rapid response of the beach striving for equilibrium shortly after nourishment, a more detailed assessment of the impacts of waves on the replenished beach was carried out based on offshore wave power during discrete periods between beach surveys. Average and cumulative wave power were calculated from wave data recorded at the Sandettie Lightship buoy for each period between two consecutive topographical surveys (Fig. 10b) and were compared with net and gross volume changes measured during the same time period (Fig. 10a). Because the length of the different time periods is very variable, being comprised between 10 and

Fig. 10 **a** Gross and net volume changes measured in area 1 (see Fig. 2 for location), and **b** average ($\overline{P}$) and cumulative (P_c) wave power between consecutive beach surveys. See text for explanation

195 days, cumulative wave power values are of course extremely different from one period to another, ranging from 0.52×10^3 kW m^{-1} (June to July 2016) to 20.6×10^3 kW m^{-1} (October 2014 to February 2015) (Fig. 10b). Nevertheless, even the average wave period during each beach survey period significantly varied during the 2½ year period of the study, ranging from 1.1 kW m^{-1} (June to July 2016) to 16.7 kW m^{-1} (November 2015).

Linear regression analyses showed no relationships between average wave power ($\overline{P}$) and either net ($R^2 = 0.01$) or gross ($R^2 = 0.07$) beach volume change (Fig. 11 a & b). Much more significant relationships were obtained when comparing cumulative wave power (P_c) with beach volume change (Fig. 11 c & d), which shows that the beach morphological variations are better explained by the total wave energy expenditure during a distinct period rather than by the mean wave energy level during the same period. Although longer time periods lead to higher P_c values and allow for more substantial beach change, our results nevertheless suggest that during periods of similar mean wave energy, the morphological variation of the beach occurs mostly in response to high energy events rather than to waves of similar energy. The strongest relationship ($R^2 = 0.87$) was observed between P_c and gross volume change (Fig. 11d) that takes into account the total variations in beach surface elevation (either positive or negative) across the nourishment area. This shows that gross volume change better reflects the morphological response of the beach to wave energy fluctuations rather than net volume changes since small net changes can be the result of significant erosion in one part of the beach and deposition in other parts.

The possible influence of the direction of the incident waves on the morphological response of the beach was also assessed. Since the wave data recorded at the Sandettie Lightship buoy are non-directional, wind directions were used as proxy for offshore wave directions, enabling to discriminate between westerly (225°-315°) and northerly (315°-45°) waves. Because only comparison between P_c and volume change gave statistically significant results (Fig. 11), only P_c was used for evaluating the possible influence of wave directions on beach volume change. Our results show significant relationships between P_c and volume change for all wave directions, but higher correlation coefficients were obtained when considering waves during northerly wind conditions (Fig. 12), comparatively to waves during westerly winds, demonstrating that the beach responds more significantly to waves originating from the north.

Discussion

Although the implantation of hard coastal defence structures has traditionally been the preferred strategy for stabilizing the shoreline in France (Anthony and Sabatier, 2012), the use of beach nourishment as a mean of coastal protection increased during the last decades even if such practice is still restricted to a limited number of sites (Anthony et al., 2011; Pupier-

Fig. 11 Relationship between the average wave power and (**a**) net beach volume change and (**b**) gross beach volume change, and between cumulative wave power and (**c**) net beach volume change and (**d**) gross beach volume change
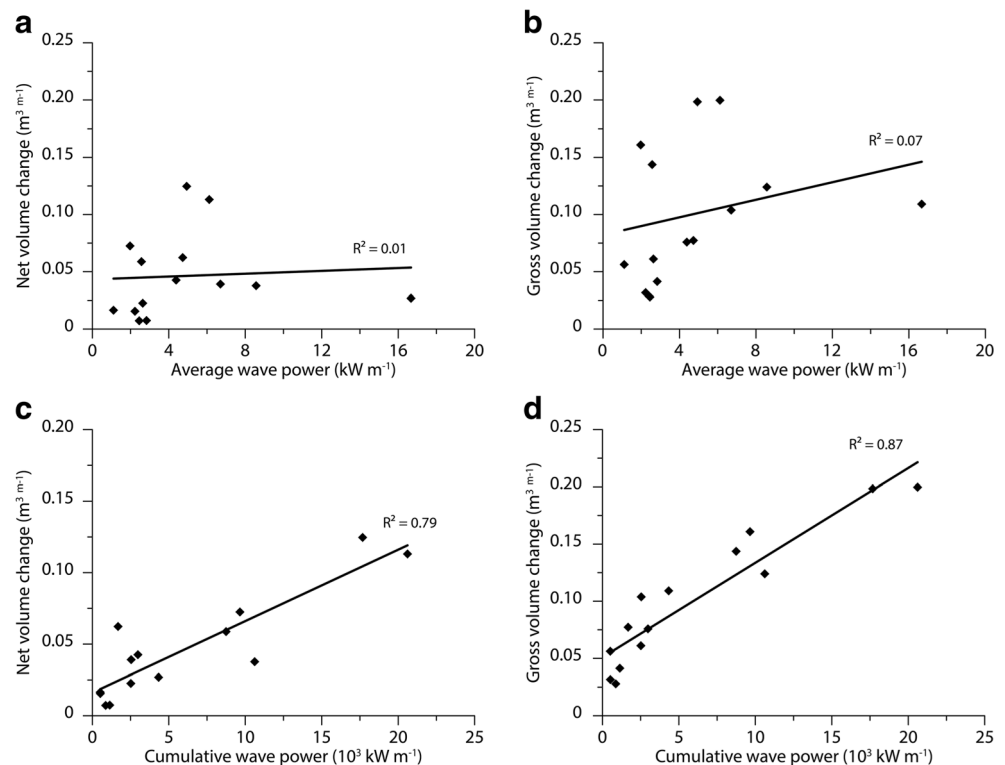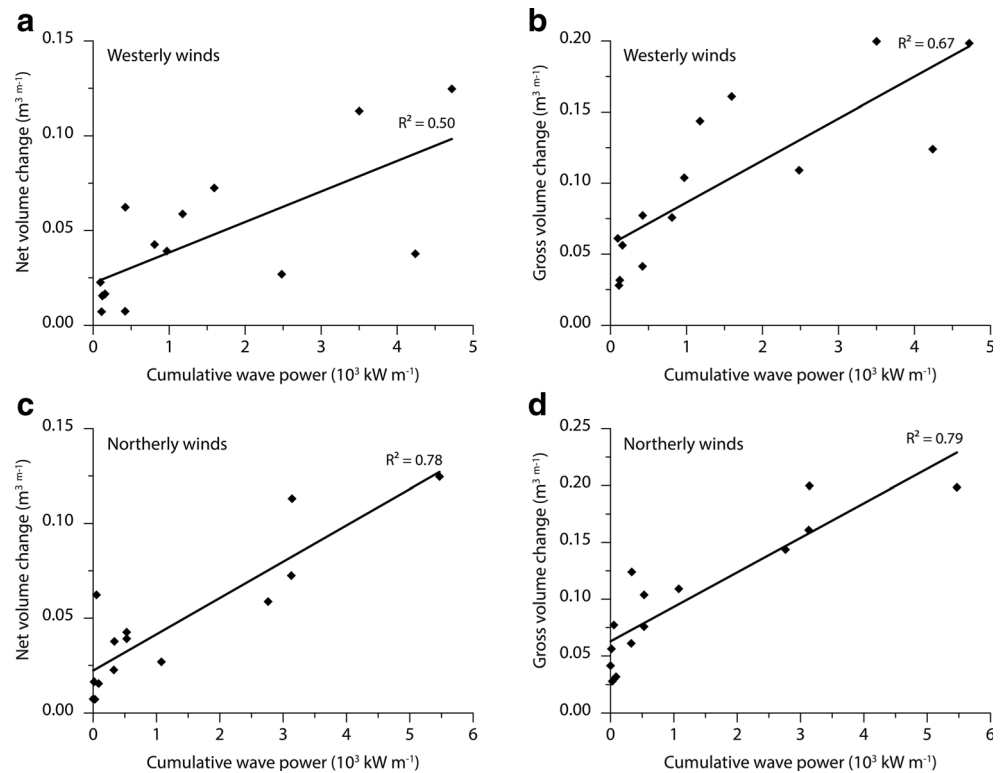
Fig. 12 Relationship between cumulative wave power and beach volume change (net and gross) during (**a** & **b**) westerly wind conditions, and (**c** & **d**) northerly wind conditions

Dauchez, 2002; Vanroye, 2008). This increase in the implementation of beach nourishment project is possibly related to an increasing awareness of the value of natural systems and of the natural mobility of beaches (Benedet et al., 2016), but also because beach nourishment preserves the aesthetic and recreational values of the replenished beaches that represent a valuable socio-economic asset. Yet, this method still encounters strong opposition at local and regional levels because of questions about the actual performance of beach nourishments.

Significant losses of sediment can take place shortly after the completion of beach replenishment projects, sometimes within a time-frame of a few months, as documented in numerous studies (e.g., Leonard et al., 1990a; Psuty and Moreira, 1992; Marcomini and Lopez, 2006; Andrade et al., 2006; van Rijn, 2011; de Schipper et al., 2014). Sediment loss was observed after the beach nourishment in front of the *Digue des Alliés* dike, but beach erosion slightly decreased during the second year albeit higher wave energy conditions during that time period, possibly reflecting an initial phase of rapid readjustment of the beach shape towards equilibrium. In their study of the evolution of a beach replenishment at Vlugtenburg on the Dutch coast, de Schipper et al. (2015) showed that 70% of the sand that was lost during the first 3½ years was eroded during the first few months after the end of the nourishment operations. According to the National Research Council (NRC, 1995), a significant loss of the sand placement generally occurs immediately after beach nourishment due to rapid morphodynamic

readjustment. In the case of the beach nourishment in front of the *Digue des Alliés*, the loss of about −138,000 m³ two years after the end of the nourishment, representing about 9% of the total nourishment volume, attests the stability of the sand placement. In addition, our measurements show that 70% of the sand eroded during the second year after nourishment was not lost, but redistributed eastward to downdrift sections of the beach. Longshore redistribution of nourishment sand can sometimes be a major objective of a beach replenishment scheme, like the Sand Motor on the Dutch coast (de Schipper et al., 2016) that was specifically designed for this purpose. In such case, a local decrease of the volume of the sand placement is not necessarily detrimental. The regular monitoring of the volume of sand of the beach at Atlantic City in New Jersey after beach nourishment operations in 1963 and 1970 showed that the sand volume rapidly decreased at the beach fill site after each nourishment, but that the rest of the beach progressively gained sediments downdrift during the following years (Everts et al., 1974). On that beach, several years were necessary for the sand to be redistributed along the coast at a distance of about 2 km from the nourishment site.

Our hydrodynamic measurements on the beach and in the nearshore zone seaward of the *Digue des Alliés* clearly showed that sediments are mostly transported eastward in response to eastward-directed wave-induced currents and flood-dominated tidal currents, which corresponds to previous observations in the area (Héquette et al., 2008a; Cartier and Héquette, 2011). Our results nevertheless suggest that tidal

currents alone cannot be responsible for the transport of significant quantities of sediment, especially on the beach where waves and wave-induced currents are the main mechanism of sediment remobilization (Figs. 7 b&f). Not only bed shear stress increases significantly on the beach with increasing wave heights (Fig. 7f), enhancing sediment resuspension, but currents are stronger during these higher energy conditions (Fig. 7d). Although this likely results in a significant increase in longshore sediment transport, some sediment is probably also dispersed seaward by bed return flows during stormy conditions as shown by our hydrodynamic measurements (Fig. 8b). Once transported offshore to the nearshore zone, these sediments are probably lost for the nourished beach as they are presumably transported alongshore by predominantly alongshore-oriented shoreface currents (Héquette et al., 2008a). Such offshore diffusion of the nourishment sands could explain the observed discrepancy between the volume of sand eroded from the nourishment area and the smaller volume of sand deposited on the remaining part of the beach.

As mentioned earlier, the strength of tidal currents decreases from the nearshore to the beach (Fig. 7d), but also from the lower to the upper beach as shown by hydrodynamic measurements carried out across the intertidal zone of several beaches of the region (Reichmüth and Anthony, 2007; Cartier and Héquette, 2013). Therefore, the morphological evolution of the supratidal platform, which can only be submerged during high wave-energy events associated with significant storm surges, is essentially controlled by wave-induced processes. Our results shows that the edge of the supratidal platform retreated landward in the western part of the beach fill due to beach erosion and landward translation of the beach profile (Fig. 6). Analyses of wave power and beach volume change indicate that the largest variations in beach volume mainly occurred during periods of high wave energy that mainly corresponded to the winter months (Fig. 10). Following the approach of de Schipper et al. (2016) who analyzed the relationships between offshore wave power and the volume change of the Sand Engine nourishment, we obtained the best fit relationship between cumulative wave power (P_c) and gross volume change gave change (V_g) ($R^2 = 0.87$) while a slightly lower correlation was found between (P_c) and net volume change (V_n). ($R^2 = 0.79$) (Fig. 11). These results are very similar to the ones reported by de Schipper et al. (2016) who found correlation coefficients (R^2) of 0.81 and 0.72 between P_c and V_g and between P_c and V_n.respectively. Our analyses also showed that the beach response is also sensitive to wave direction, with stronger relationships between P_c and beach volume change when computing wave power during northerly wind conditions comparatively to westerly winds (Fig. 12), suggesting that waves have stronger impacts on the beach when waves originate from the north. These results echo the findings of Ruz et al. (2009) that beach and coastal dune erosion along North Sea facing coast of norther France is strongly linked with the occurrence of sustained winds from the northern quadrant responsible for the generation of incident waves with an initial shore-normal direction.

The cross-shore morphological response of the beach profiles in the nourishment area also logically showed a strong link with wave forcing, with more significant changes observed after high energy events during winter (Fig. 6 b & c). This evolution strongly suggests that profile equilibration after the nourishment was essentially an event-driven mechanism rather than a progressive gradual adjustment of the beach profile towards a new state of dynamic equilibrium. Our results are therefore similar to those obtained by Wang et al. (2003), Elko and Wang (2007) and by de Schipper et al. (2012) on other replenished beaches who found that the rate at which beach morphology evolves after nourishment is a function of wave energy rather than time, which contradicts the concept of a long-term gradual profile equilibration (Browder and Dean, 2000; Dean, 2002).

Conclusion

The aim of this paper was to assess the efficiency of a massive beach nourishment project after a period of 2 ½ years and to evaluate the impacts of hydro-meteorological forcings on the observed morphological changes. Our results highlight the key role of waves in the morphological evolution of the site, especially during winter periods due to higher energy conditions. Our results also underline that northerly waves, which have a more direct incidence towards the beach, had stronger impacts on the replenished beach rather than the prevailing westerly waves. The morphological evolution of the nourished beach shows that beach erosion tended to decrease after an initial phase of rapid readjustment of the beach shape towards equilibrium. The supratidal sandy platform created in 2014 continues today to insure the protection of the dike by constituting a buffer zone that is still efficient for limiting flood hazards. After about 2 years, only 9.2% of the initial beach nourishment volume was lost, representing a loss of −138,200 m³, and most of the eroded material was partly redistributing downdrift as predicted by numerical modelling. The seaside resort of Malo-les-Bains takes advantage of the progressive dispersal of sand from the nourishment zone to the beach located downdrift. This operation has, thus far, been a successful example of massive beach nourishment from beneficial reuse of clean dredging sand for coastal protection purposes. In accordance with the strategy of the Port of Dunkirk for a sustainable management of sediment, this project demonstrates the opportunity to combine dredged sand from navigation channel and the protection of a key structure for people safety with regard to marine flooding.

References

Andrade C, Lira F, Pereira MT et al (2006) Monitoring the nourishment of Santo Amaro estuarine beach (Portugal). J Coast Res SI 39:776–782

Anthony EJ, Sabatier F (2012) Coastal stabilization practices in France. In: JAG C, Pilkey OH (eds) pitfalls of shoreline stabilization. Coastal research library 3. Springer, Netherlands, pp 303–321

Anthony EJ, Cohen O, Sabatier F (2011) Chronic offshore loss of nourishment on nice beach, French Riviera: a case of over-nourishment of a steep beach? Coast Eng 58:374–383

Bakker MAJ, van Heteren S, Vonhögen LM, van der Spek AJF, van der Valk B (2012) Recent coastal dune development: effects of sand nourishments. J Coast Res 28:587–601

Benedet L, Dobrochinski JPF, Walstra DJR, Klein AHF, Ranasinghe R (2016) A morphological modeling study to compare different methods of wave climate schematization and evaluate strategies to reduce erosion losses from a beach nourishment project. Coast Eng 112:69–86

Bertin X, Prouteau E, Letetrel C (2013) A significant increase in wave height in the North Atlantic Ocean over the 20th century. Glob Planet Chang 106:77–83

Bird E, Lewis N (2015) Beach renourishment. Springer, Dordrecht

Browder AE, Dean RG (2000) Monitoring and comparison to predictive models of the Perdido key beach nourishment project, Florida, USA. Coast Eng 39:173–191

Brown S, Nicholls R, Woodroffe C et al (2013) Sea-level rise impacts and responses: a global perspective. In: Finkl CW (ed) Coastal Hazards. Springer, Netherlands, pp 117–149

Cai F, Dean RG, Liu J (2010) Beach nourishment in China: status and prospects. In: Smith JM, Lynett P (eds) Proceedings of the 32nd conference on coastal engineering, shanghai, June 30-July 5 2010, pp 3753–3764

Campbell TJ, Benedet L (2006) Beach nourishment magnitudes and trends in the US. J Coast Res SI 39:57–64

Cartier A, Héquette A (2011) Estimation of longshore and cross shore sediment transport on sandy macrotidal beaches of northern France. In: Rosati JD, Wang P, Roberts TM (eds) proceeding of the coastal sediments 2011, Miami, 2-6 may 2011, pp 2130–2143

Cartier A, Héquette A (2013) The influence of intertidal bar-trough morphology on sediment transport on macrotidal beaches, northern France. Z Geomorphol 57:325–347

Cartier A, Tresca A, Grunnet N, Michard B, Forain N, Vial T (2014) Confortement d'un ouvrage de prevention des inondations et des submersions marines: l'exemple de la digue des Alliés à Dunkerque. XIIIèmes Journées Nationales Génie Côtier Génie Civil, Dunkirk, 2-4 July 2014, pp 641–648

Charlier RH, Chaineux MCP, Morcos S (2005) Panorama of the history of coastal protection. J Coast Res 21:79–111

Charlier RH, De Meyer CP (1995) New developments on coastal protection along the Belgian coast. J Coast Res 11:1287–1293

Cooke BC, Jones AR, Goodwin ID, Bishop MJ (2012) Nourishment practices on Australian sandy beaches: a review. J Environ Manag 113:319–327

Crapoulet A, Héquette A, Levoy F, Bretel P (2016) Using LiDAR topographic data for identifying coastal areas of northern France vulnerable to sea-level rise. J Coast Res SI 75:1067–1071

Dean RG (2002) Beach nourishment: theory and practice. World Scientific, River Edge, NJ

Dean RG, Houston JR (2016) Determining shoreline response to sea level rise. Coast Eng 114:1–8

de Schipper MA, de Vries S, Ranasinghe R et al (2012) Morphological developments after a beach and shoreface nourishment at Vlugtenburg beach. In: Kranenburg WM and Horstman EM and Wijnberg KM (eds) NCK-days 2012: crossing borders in coastal research, Enschede, 13-16 March 2012, pp 115–118

de Schipper MA, de Vries S, Stive MJF et al (2014) Morphological development of a mega-nourishment: first observations at the sand engine. In: Lynett PJ (ed) Proceedings of the 34th international conference on coastal engineering, Seoul, 14-20 June 2014

de Schipper MA, de Vries S, Mil-Homens J et al (2015) Initial volume losses at nourished beaches and the effect of surfzone slope. In: Wang P, Rosati JD, Cheng J (eds) Proceedings of the coastal sediment 2015, San Diego, 11-15 May 2015

de Schipper MA, de Vries S, Ruessink G et al (2016) Initial spreading of a mega feeder nourishment: observations of the sand engine pilot project. Coast Eng 111:23–38

DHI (2012) Etudes hydrauliques et de conception d'un dispositif de confortement de la Digue des Alliés – Final report by Danish Hydraulic Institute, p 469

Elko NA, Wang P (2007) Immediate profile and planform evolution of a beach nourishment project with hurricane influences. Coast Eng 54:49–66

Everts CH, DeWall AE, Czerniak MT (1974) Behavior of beach fill at Atlantic City, New Jersey. In: Proceedings of the 14th international conference on coastal engineering Copenhague, 24-28 June 1974, pp 1370–1388

GPMD (2012) Topo-bathymetric data of the beach nourishment of the Digue des Alliés. Internal technical report – Grand Port Maritime de Dunkerque. Dunkirk, CD-rom

Grant WD, Madsen OS (1986) The continental shelf bottom boundary layer. Ann Rev Fluid Mech 18:265–305

Grunnet N, Kristensen SE, Drønen N et al (2012) Evaluation of nourishment schemes based on long-term morphological modeling. In: Lynett P, Smith JM (eds) Proceedings of the 33rd conference on coastal engineering, Santander, 1-6 July 2012

Guimaraes A, Lima M, Coelho C, Silva R, Veloso-Gomes F (2016) Groin impacts on updrift morphology: physical and numerical study. Coast Eng 109:63–75

Haigh I, Nicholls R, Wells N (2011) Rising sea levels in the English Channel 1900 to 2100. Mar Eng 164:81–92

Hall Jr JV (1952) Artificially nourished and constructed beaches. In: Johnson JW (ed) Proceedings of the 3rd conference on coastal engineering, Cambridge, pp 119-136

Hamm L, Capobianco M, Dette HH et al (2002) A summary of European experience with shore nourishment. Coast Eng 47:237–264

Hanson H, Brampton A, Capobianco M, Dette HH, Hamm L, Laustrup C, Lechuga A, Spanhoff R (2002) Beach nourishment projects, practices, and objectives-a European overview. Coast Eng 47:81–111

Héquette A, Cartier A (2016) Theoretical and observed breaking wave height on a barred macrotidal beach: implications for the estimation of breaker index on beaches with large tidal range. J Coast Res SI 75:861–866

Héquette A, Hemdane Y, Anthony EJ (2008a) Sediment transport under wave and current combined flows on a tide-dominated shoreface, northern coast of France. Mar Geol 249:226–242

Héquette A, Hemdane Y, Anthony EJ (2008b) Determination of sediment transport paths in macrotidal shoreface environments: a comparison of grain-size trend analysis with near-bed current measurements. J Coast Res 24:695–707

HydroConsult (2011) Topographic and bathymetric survey – technical report for port of Dunkirk, Digue des Alliés. DVD-rom

IPCC (2013) Climate change 2013: the physical science basis. Contribution of working group I to the fifth assessment report of the intergovernmental panel on climate change. TF stocker et al. (eds) Cambridge University press, Cambridge, p 1535

Kabat P, Fresco LO, Stive MJF et al (2009) Dutch coasts in transition. Nat Geosci 2:450–452

Kamphuis JW (2010) Introduction to coastal engineering and management, 2nd edition. Advance series on Ocean engineering, vol 30. World Scientific, Singapore

Koch EW, Barbier EB, Silliman BR et al (2009) Non-linearity in ecosystem services: temporal and spatial variability in coastal protection. Front Ecol Environ 7:29–37

Kruel S (2016) The impacts of sea-level rise on tidal flooding in Boston, Massachusetts. J Coast Res 32:1302–1309

Leonard L, Clayton T, Pilkey OH (1990a) An analysis of Replenished Beach design parameters on U.S. East Coast Barrier Islands. J Coast Res 6:15–36

Leonard L, Dixon KL, Pilkey OH (1990b) A comparison of beach replenishment on the U.S. Atlantic, Pacific, and Gulf coasts. J Coast Res SI 6:127–140

Le Louarn P (2012) Le droit dans la tempête. Norois 222:61–77

Maspataud A, Ruz M-H, Vanhée S (2013) Potential impacts of extreme storm surges on a low-lying densely populated coastline: the case of Dunkirk area, northern France. Nat Hazards 66:1327–1343

Marcomini SC, López RA (2006) Evolution of a beach nourishment project at mar del Plata. J Coast Res SI 39:834–837

McRobie A, Spencer T, Gerritsen H (2005) The big flood: North Sea storm surge. Philos Transact A Math Phys Eng Sci 363:1263–1270

Mertens T, De Wolf P, Verwaest T et al (2008) An integrated master plan for Flanders future coastal safety. In: Smith JM (ed) Proceedings of the 31st conference of coastal engineering, Hamburg, 31 august-5 September 2008, pp 4017–4028

Muñoz-Perez JJ, Lopez de San Roman-Blanco B, Gutierrez-Mas JM, Moreno L, Cuena GJ (2001) Cost of beach maintenance in the Gulf of Cadiz (SW Spain). Coast Eng 42:143–153

National Research Council (1995) Beach nourishment and protection. National Academies Press, Washington

Neumann B, Vafeidis AT, Zimmermann J, Nicholls RJ (2015) Future coastal population growth and exposure to sea-level rise and coastal flooding - a global assessment. PLoS One 10. doi:10.1371/journal.pone.0118571

Nicholls RJ, Cazenave A (2010) Sea-level rise and its impact on coastal zones. Science 328:1517–1520

Oblinger A, Anthony EJ (2008) Wave attenuation and intertidal morphology of a multi-barred macrotidal beach behind a breakwater. Z Geomorphol Suppl 52(3):167–177

Psuty NP, Moreira MES (1992) Characteristics and longevity of beach nourishment at Praia da Rocha, Portugal. J Coast Res 8:660–676

Pupier-Dauchez S (2002) Le rechargement sédimentaire: de la défense des côtes à l'aménagement du littoral : Analyse des pratiques sur la côte atlantique française. PhD dissertation, Université de Bretagne occidentale

Rahmstorf S, Perrette M, Vermeer M (2012) Testing the robustness of semi-empirical sea level projections. Clim Dynam 39:861–875

Reichmüth B, Anthony EJ (2007) Tidal influence on the intertidal bar morphology of two contrasting macrotidal beaches. Geomorphology 90:101–114

Roelse P (1990) Beach and dune nourishment in the Netherlands. In: Edge BL (ed) Proceedings of the 22nd coastal engineering, Delft, pp 1984–1997

Rufin-Soler C, Héquette A, Gardel A (2008) Assessing the vulnerability of coastal lowlands to marine flooding using LIDAR data, Sangatte coastal dunes, northern France. Z Geomorphol Suppl 52(3):195–211

Ruggiero P (2013) Is the intensifying wave climate of the U.S. Pacific northwest increasing flooding and erosion risk faster than sea-level rise? J Waterw Port C-ASCE 139:88–97

Ruz M-H, Anthony EJ, Faucon L (2005) Coastal dune evolution on a shoreline subject to strong human pressure: the Dunkirk area, northern France. In: Herrier JL, Mees J, Salman a, Seys J, van Nieuwenhuyse H, Dobbelaere I (eds) Proceedings 'dunes and estuaries 2005' – international conference on nature restoration practices in European coastal habitats, Koksijde, Belgium, 19-23 September 2005, pp 441–449

Ruz M-H, Héquette A, Maspataud A (2009) Identifying forcing conditions responsible for foredune erosion on the northern coast of France. J Coast Res SI 56:356–360

Sánchez-Badorrey E, Losada MA, Rodero J (2008) Sediment transport patterns in front of reflective structures under wind wave-dominated conditions. Coast Eng 55:685–700

Shibutani Y, Matsubara Y, Kuroiwa M (2013) Effect of the coastal conservation due to beach nourishment of Totori sand dune coast. In: Suriamihardja DA, Harianto T, Abdurrahman MA, Rachman T (eds) Proceedings of the 7th international conference on Asian and Pacific coasts, Bali, 24−26 September 2013, pp 79–84

Silveira TM, Santos CF, Andrade F (2013) Beneficial use of dredged sand for beach nourishment and coastal landform enhancement-the case study of Tria, Portugal. J Coast Conser 17:825–832

Speybroeck J, Bonte D, Courtens W et al (2006) Beach nourishment: an ecologically sound coastal defence alternative? A review. Aquat Conserv 16:419–435

Stive MJF, de Schipper MA, Luijendijk AP et al (2013) A new alternative to saving our beaches from sea-level rise: the sand engine. J Coastal Res 29:1001–1008

Temmerman S, Meire P, Bouma TJ et al (2013) Ecosystem-based coastal defence in the face of global change. Nature 504:79–83

Trembanis AC, Pilkey OH (1998) Summary of beach nourishment along the U.S. Gulf of Mexico shoreline. J Coastal Res 14:407–417

Valverde HR, Trembanis AC, Pilkey OH (1999) Summary of beach nourishment episodes on the U.S. East Coast Barrier Islands. J Coast Res 15:1100–1118

van Duin MJP, Wiersma NR, Walstra DJR, van Rijn LC, Stive MJF (2004) Nourishing the shoreface: observations and hindcasting of the Egmond case, The Netherlands. Coast Eng 51:813–837

Van Rijn LC (2011) Coastal erosion and control. Ocean Coast Manag 54:867–887

Vanroye C (2008) La protection du littoral du Golfe d'Aigues-Mortes. In: Levacher D, Sanchez M (eds) Proceedings in the 10th Journ Natl Génie Côtier–Génie Civil, Sables d'Olonne, pp 14–16

Wang P, Ebersole BA, Smith ER (2003) Beach-profile evolution under spilling and plunging breakers. J Waterw Port Coast Ocean Eng 129:41–46

Weisse R, von Storch H, Niemeyer HD, Knaack H (2012) Changing North Sea storm surge climate: an increasing hazard? Ocean Coast Manag 68:58–68

Wiegel RL (1994) Ocean beach nourishment on the USA Pacific coast. Shore & Beach 62:11–36